Biogeosciences, 21, 5247–5260, 2024
https://doi.org/10.5194/bg-21-5247-2024

Biogeosciences Open Access EGU

Tidal influence on carbon dioxide and methane fluxes from tree stems and soils in mangrove forests

Zhao-Jun Yong[1,2], **Wei-Jen Lin**[1,2,3,4], **Chiao-Wen Lin**[3,4], **and Hsing-Juh Lin**[1,2,5]

[1]Department of Life Sciences, National Chung Hsing University, Taichung 40227, Taiwan
[2]Innovation and Development Center of Sustainable Agriculture,
National Chung Hsing University, Taichung 40227, Taiwan
[3]Department of Marine Environment and Engineering, National Sun Yat-sen University, Kaohsiung 80424, Taiwan
[4]The Center for Water Resources Studies, National Sun Yat-sen University, Kaohsiung 80424, Taiwan
[5]Institute of Marine Environment and Ecology, National Taiwan Ocean University, Keelung 202301, Taiwan

Correspondence: Hsing-Juh Lin (hjlin@dragon.nchu.edu.tw)

Received: 23 February 2024 – Discussion started: 26 February 2024
Revised: 24 August 2024 – Accepted: 6 October 2024 – Published: 26 November 2024

Abstract. Mangroves are critical blue carbon ecosystems. Measurements of methane (CH_4) emissions from mangrove tree stems have the potential to reduce uncertainty in the capacity of carbon sequestration. This study is the first to simultaneously measure CH_4 fluxes from both stems and soils throughout tidal cycles. We quantified carbon dioxide (CO_2) and CH_4 fluxes from mangrove tree stems of *Avicennia marina* and *Kandelia obovata*, which have distinct root structures, during tidal cycles. Tree stems of both species served as net CO_2 and CH_4 sources. Compared to fluxes in the soils, the mangrove tree stems exhibited remarkably lower CH_4 fluxes but no difference in CO_2 fluxes. The stems of *A. marina* exhibited an increasing trend in CO_2 flux from low to high tides. However, CH_4 fluxes showed high temporal variability, with the stems of *A. marina* functioning as a CH_4 sink before tidal inundation and becoming a source after ebbing. In contrast, the stems of *K. obovata* showed no consistent pattern in the CO_2 or CH_4 fluxes. Based on our findings, the stem CH_4 fluxes in *A. marina* may vary by up to 1200 % when considering tidal influence, compared to when tidal influence is ignored. Therefore, sampling only during low tides might underestimate stem CO_2 and CH_4 fluxes on a diurnal scale. This study highlights the necessity of considering tidal influence and species when quantifying greenhouse gas (GHG) fluxes from mangrove tree stems. Further study is needed to explore the underlying mechanisms driving the observed flux variations and improve the understanding of GHG dynamics in mangrove ecosystems.

1 Introduction

Global methane (CH_4) emissions have reached a record-high level (Saunois et al., 2020). Currently, there are two primary methods utilized for assessing global CH_4 emissions: the bottom-up method and the top-down method. The bottom-up method relies on compiling data from greenhouse gas (GHG) inventories and biogeochemical models to infer the sources of emissions. On the other hand, the top-down method involves measuring atmospheric CH_4 concentrations and utilizing transport models to infer the sources of emissions in order to estimate and assess CH_4 emissions on a global scale. CH_4 emissions estimated by the bottom-up method are significantly higher than those estimated by the top-down method, indicating a high degree of uncertainty and suggesting that some sources may be overlooked or not well understood (Jackson et al., 2020). CH_4 generated in wetlands can be released into the atmosphere not only through diffusion, ebullition, and transport mediated by herbaceous plants but also through the stems of woody plants (Gauci et al., 2010; Terazawa et al., 2007). Pangala et al. (2017) demonstrated that the difference between top-down and bottom-up estimates of CH_4 emissions could be accounted for by the upscaled CH_4 flux from tree stems, emphasizing the necessity of considering this pathway in carbon budgets (Carmichael et al., 2014). Furthermore, forest wetlands account for approximately 60 % of the global wetland area, highlighting the potential contribution of woody stems to global GHG emissions

(Barba et al., 2019a; Covey and Megonigal, 2019). While carbon dioxide (CO_2) exchange at the stem–atmosphere interface has been examined (Teskey et al., 2008), little is known regarding the sources and mechanisms of CH_4 emissions originating from tree stems relative to those originating from other pathways. CH_4 emitted by tree stems may originate from microorganisms/cryptogams within the stem bark (Jeffrey et al., 2021; Lenhart et al., 2015) or from the soil, where it is produced and enters the roots before being transported in either liquid or gaseous form through xylem or aerenchyma tissue (Kutschera et al., 2016; Vroom et al., 2022).

GHG emissions from tree stems exhibit temporal and spatial variations, with different influencing mechanisms found in various studies. Firstly, tree stem GHG fluxes tend to be higher during the growing season and lower during the dormant season, but there may also be no significant differences among seasons (Barba et al., 2019b; Köhn et al., 2021; Pangala et al., 2015; Pitz et al., 2018; Wang et al., 2016; Zhang et al., 2022). Secondly, significant variations in GHG fluxes from tree stems have been observed at different heights above ground level, with a decreasing trend along the tree stem height (Moldaschl et al., 2021; Pangala et al., 2013, 2014, 2015; Sjögersten et al., 2020), although some studies have not reported this phenomenon (Machacova et al., 2021; Wang et al., 2016). Thirdly, tree stem GHG emissions may be regulated by various environmental factors, such as temperature, moisture, and redox potential (Barba et al., 2019b; Gao et al., 2021; Jeffrey et al., 2019; Pitz et al., 2018; Schindler et al., 2020, 2021; Sjögersten et al., 2020; Terazawa et al., 2015), which can be affected by fluctuations in water table height due to seasonal changes and hydrological processes (Jeffrey et al., 2023; Peacock et al., 2024; Terazawa et al., 2021). Finally, the physiological factors of trees, such as lenticel density, wood density, water content, and stem bark structure, may also influence GHG fluxes originating from tree stems (Jeffrey et al., 2024; Pangala et al., 2013, 2014, 2015; Wang et al., 2016; Zhang et al., 2022).

However, most related studies have focused on freshwater wetlands and upland forests, while relatively limited research has focused on mangrove forests. Jeffrey et al. (2019) reported that dead mangrove trees may account for approximately 26 % of CH_4 emissions in mangrove ecosystems. However, He et al. (2019) reported inconsistent results, revealing a relatively small contribution from tree stems. The contribution of mangrove tree stems to the ecosystem GHG flux is generally less than the contribution of soil (Gao et al., 2021; He et al., 2019; Jeffrey et al., 2019), but it still has the potential to exceed 50 % (Zhang et al., 2022). Additionally, GHG fluxes from mangrove tree stems vary among tree species (Zhang et al., 2022) and may even differ within a single tree species (Gao et al., 2021), highlighting the uncertainty in GHG emissions from mangrove tree stems and emphasizing the need for further investigation.

Mangroves are primarily distributed in tropical and subtropical coastal regions and are regarded as critical ecosystems with a high capacity for sequestering blue carbon (Li et al., 2018; Duarte de Paula Costa and Macreadie, 2022). The anaerobic conditions resulting from tidal inundation, along with the abundant organic matter, turn mangrove soil into a source of CH_4 emissions (Lin et al., 2020). This, in turn, impacts their role in mitigating global warming. Moreover, several studies have demonstrated the influence of tides on the emission of GHGs in coastal wetlands. In both seagrass meadows and tidal marshes, the CH_4 flux tends to peak when tidal water reaches the sampling site (Bahlmann et al., 2015; Capooci and Vargas, 2022). The sudden release of CH_4 can occur through physical force under the influence of tidal movement (Li et al., 2021), resulting in the advective exchange of groundwater or soil pore water with the overlying surface water (Billerbeck et al., 2006; Rosentreter et al., 2018). CH_4 emissions during tidal inundation may be higher if tidal water contains high concentrations of dissolved CH_4, which can increase the emissions of CH_4 through diffusion due to the concentration gradient (Sturm et al., 2017; Tong et al., 2013). Yamamoto et al. (2009) reported a positive correlation between the water table and GHG fluxes in the flooded littoral zone with vegetation, suggesting that water pressure, rather than gas diffusion, primarily affects the emissions of CO_2 and CH_4 across the water–atmosphere interface by ejecting gases from pore spaces. This finding is contrary to previous results in which lower CH_4 fluxes were observed during high tides, which may have been caused by the higher water pressure limiting CH_4 diffusion in soil pore spaces filled with water and plant-mediated transport (Tong et al., 2010, 2013). Additionally, CH_4 may be oxidized during diffusion in water (Tong et al., 2013). Furthermore, if the dissolved oxygen concentration, sulfate concentration, and salinity are high in tidewater, this may inhibit CH_4 production and/or promote CH_4 oxidation (Huang et al., 2019), resulting in lower CH_4 emissions during high tides. The variation in the CH_4 flux across the water–atmosphere interface during tidal inundation could be driven by current- or wind-induced turbulence (Sturm et al., 2017). CH_4 emissions even exhibited different trends during spring and neap tides (Huang et al., 2019; Tong et al., 2013). However, to our knowledge, there is only one study on GHG fluxes from mangrove tree stems during tidal cycles (Epron et al., 2023).

This study aimed to quantify the CO_2 and CH_4 emissions from the tree stems of *K. obovata* and *A. marina*, which are dominant mangrove species with distinct root structures, distributed along the northern and southern coasts of Taiwan, respectively. We investigated the temporal variations in stem GHG fluxes during tidal cycles and assessed the influence of tides on the upscaled flux. We also simultaneously measured the GHG emissions from mangrove soil, even during tidal inundation, to compare the temporal dynamics of GHG fluxes between the tree stems and soil. We hypothesized that GHG fluxes from mangrove tree stems and soil exhibit syn-

chronized temporal and species variation during the tidal cycle and that the tidal cycle may exert a significant impact on GHG emissions on a larger scale.

2 Materials and methods

2.1 Site description

This study focused on mangroves at four sites along the western coast of Taiwan (Fig. 1). The dominant mangrove species in Wazihwei (K-WZW; 25°10′ N, 121°25′ E) and Xinfeng (K-XF; 24°55′ N, 120°58′ E) is *Kandelia obovata*, while *Avicennia marina* is the dominant species in Fangyuan (A-FY; 23°56′ N, 120°19′ E) and Beimen (A-BM; 23°17′ N, 120°6′ E). K-WZW and K-XF are situated in northern Taiwan, a subtropical region, with average annual precipitation values of 2023 and 1537 mm, respectively. A-FY and A-BM are located in southern Taiwan, a tropical region, with average annual precipitation values of 1162 and 1603 mm, respectively. A-BM has the largest forest area (75.3 ha), while K-XF has the smallest (8.12 ha). Mean tree height across all sites ranged from 1.8 to 5.1 m, and tree density and diameter at breast height (DBH) averaged 0.6–2.4 tree m^{-2} and 5.6–10.5 cm, respectively (Table 1). The tides were semidiurnal at all sites. The soil texture at all sites was silty, with an average grain size of 0.046 mm. During summer (the study period), the average air temperature was 28.4 °C for *K. obovata* and 29.4 °C for *A. marina* (Lin et al., 2023). The sampling campaign was conducted from 1 June 2022 to 29 July 2022, with each site sampled for 3 d during the spring tide (Table 1). This period was chosen mainly because there is a higher GHG flux in summer compared to other seasons, as indicated by preliminary studies conducted at the same sites (Lin et al., 2020).

2.2 Flux measurements

At each sampling site, a mangrove tree was selected for tree stem CO_2 and CH_4 flux measurements obtained at approximately 110 cm above the ground. This specific height was chosen with consideration for the potential maximum tidal height, which may reach up to 80 cm above the ground (Table 1). Due to differences in stem morphology, two distinct stem chambers – a semirigid chamber and a cylindrical chamber – were used in this study to measure the GHG emissions of *K. obovata* and *A. marina*, respectively (Fig. S1 in the Supplement).

The semirigid chamber was adapted from Siegenthaler et al. (2016) and was constructed from transparent recycled polyethylene terephthalate (rPET) bottles. A plastic sheet measuring 14 cm in length and 11 cm in width was cut from a bottle, and 2 cm wide and 1.5 cm thick chloroprene rubber (CR) foam tape was attached around the edges and center of the plastic sheet. Two holes were drilled and fitted with adapters to connect the tubing, resulting in a chamber with a 16 cm^2 surface area and a 0.2 L volume. The chamber was installed on the tree stem with a strap prior to measurement and subsequently removed. The second cylindrical chamber was constructed from a 0.2 L white polypropylene (PP) bottle. A 16 cm^2 square was cut from the lid, and two small holes were drilled at the bottom of the bottle; these holes were fitted with adapters to connect the tubing. The lid was fixed to the stem and sealed with silicone prior to measurement. After each measurement, the chamber was removed, but the lid remained on the trunk (Fig. S1).

Two locations within 2 m of the sampled tree were selected to measure CH_4 and CO_2 fluxes at the soil–atmosphere and water–atmosphere interfaces during the tidal cycle, using the static chamber (Lee et al., 2011) and the floating chamber method (Lin et al., 2024), respectively. The soil chamber comprised a semicircular, transparent polymethyl methacrylate (PMMA) cover (30 cm in diameter) and a stainless steel ring (16 cm in height and 30 cm in diameter), with an adapter on the cover for connecting the tubing. The ring was pressed into the soil before the cover was placed over it, and a long-tailed clip was used to secure and cover the steel ring tightly to achieve an airtight seal (Fig. S1). During high tide, if the water level exceeded the height of the soil chamber (16 cm), the floating chamber was used (Fig. S1).

In this study, a portable gas analyzer (LI-7810 from LI-COR Biosciences, Lincoln, NE, USA) was used to simultaneously measure CO_2 and CH_4 fluxes. The chamber was connected to the analyzer through tubing, and the gas inside the chamber was drawn into the analyzer with a pump, with each measurement lasting approximately 5 min for the stem and 7 min for the soil. During the tidal cycle, stem and soil GHG fluxes were measured consistently. After each measurement was completed, the airtight sealed chamber was opened for approximately 3 min to allow the GHG concentration within the chamber to stabilize. Simultaneously, at the beginning of the flux measurement, the water level adjacent to the sampled trees was measured using a tape measure fixed to a PVC pipe (Fig. S1). To minimize soil disturbance, the researcher remained stationary at one location during the sampling campaign and avoided walking around. Sampling was mainly conducted during daylight hours. Soil GHG flux data were mainly derived from Lin et al. (2024). The GHG flux (F) was calculated using the following equation:

$$F = (S \times V \times c)/(RT \times A), \quad (1)$$

where S is the slope obtained from the linear regression of GHG concentration changes over time (expressed in ppb CH_4 s^{-1} or ppm CO_2 s^{-1}), V is the chamber volume (liters), c is the conversion factor from seconds to hours, R is the ideal gas constant (0.082 L atm K^{-1} mol^{-1}), T is the air temperature inside the chamber (kelvin), and A is the surface area of the chamber (m^2). If the R^2 value of the linear regression was < 0.7, the GHG flux was removed from further statistical analysis. The surface area and volume of the semi-

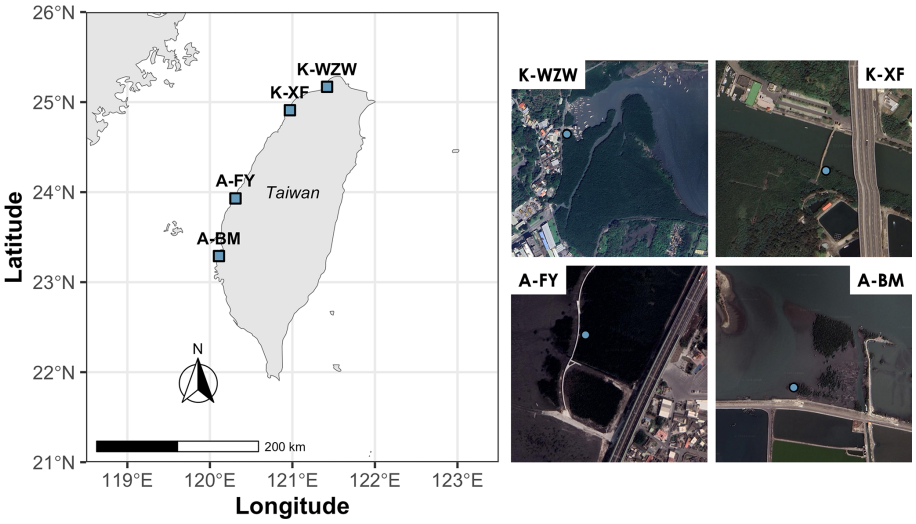

Figure 1. Sample sites along the western coast of Taiwan. The blue dots represent the locations of sampled trees. K-WZW: Wazihwei. K-XF: Xinfeng. A-FY: Fangyuan. A-BM: Beimen. The dominant mangrove species in K-WZW and K-XF is *Kandelia obovata*, while *Avicennia marina* is the dominant species in A-FY and A-BM. The map sources are Natural Earth (left) and © Google Earth (right).

rigid chamber were calculated as described by Siegenthaler et al. (2016).

Different upscaling methods were applied to the tree stem GHG fluxes. First, the average fluxes during low and high tides were multiplied by the non-inundation time and the inundation time (in hours), respectively. These values were then summed to calculate the daily fluxes, accounting for tidal influence, which is denoted as F_{BothTide}. Since sampling in mangrove forests was mostly conducted during low tide, the average fluxes during low tide were multiplied by 24 h to scale up to daily fluxes, denoted as F_{LowTide}, for comparison with the fluxes accounting for tidal influence. The equations are shown below:

$$F_{\mathrm{BothTide}} = \left(F_{\mathrm{high}} \times t_{\mathrm{inundated}}\right) + \left(F_{\mathrm{low}} \times \left(24 - t_{\mathrm{inundated}}\right)\right), \quad (2)$$

$$F_{\mathrm{LowTide}} = F_{\mathrm{low}} \times 24, \quad (3)$$

where F_{low} and F_{high} are the average fluxes during low and high tides, respectively, and $t_{\mathrm{inundated}}$ is the average inundation time per day, acquired by multiplying the hours per day when the water level was higher than 0 cm by 2 (since the tides are semidiurnal tides).

2.3 Statistical analysis

All the statistical analyses were performed using R 4.2.2 software. All the data were assessed for a normal distribution using the Shapiro–Wilk test. The Kruskal–Wallis test on ranks was used to evaluate the differences in CO_2 and CH_4 fluxes between sites. To determine which sites differed, Dunn's multiple comparison test was applied as a post hoc analysis when differences were significant ($p < 0.05$). The relationships between the CO_2 and CH_4 fluxes during rising and falling tides were analyzed using a simple linear regression model. The results were considered statistically significant when the p value was < 0.05. Data are primarily presented as the mean $\pm$ standard deviation (SD).

3 Results

During the study period, the mangrove tree stems served as net CO_2 sources, but there was distinct variation between sites (Fig. 2). In the *K. obovata* mangroves, the average CO_2 fluxes from the tree stems during the tidal cycle were 1.21 ± 0.10 mmol m^{-2} h^{-1} at the K-WZW site and 1.06 ± 0.20 mmol m^{-2} h^{-1} at the K-XF site (Fig. 2a). The stem CO_2 fluxes were significantly higher at the A-FY and A-BM sites, averaging 10.62 ± 2.35 and 16.00 ± 9.41 mmol m^{-2} h^{-1}, respectively (Fig. 2a). Across all sites, only the tree stem at the A-FY site functioned as a net CH_4 sink (-0.17 ± 0.52 µmol m^{-2} h^{-1}). However, the stem CH_4 fluxes at the K-WZW and K-XF sites showed no significant difference compared to the A-FY site, averaging 0.05 ± 0.06 and 0.04 ± 0.04 µmol m^{-2} h^{-1}, respectively (Fig. 2b). The stem CH_4 fluxes were significantly higher at the A-BM site (0.48 ± 1.17 µmol m^{-2} h^{-1}; Fig. 2b). Compared to those of the tree stems, the soils of the *K. obovata* and *A. marina* mangrove forests exhibited remarkably high CH_4 fluxes, averaging 7.59 ± 8.74 and 42.23 ± 62.95 µmol m^{-2} h^{-1}, respectively. The average CO_2 flux from the soil was 1.73 ± 2.31 mmol m^{-2} h^{-1} in the *K. obovata* mangroves and 3.42 ± 3.36 mmol m^{-2} h^{-1} in the *A. marina* mangroves, but it did not differ significantly from that of the tree stems.

The mean inundation time and highest tidal height at each sampling site are provided in Table 1. During the tidal

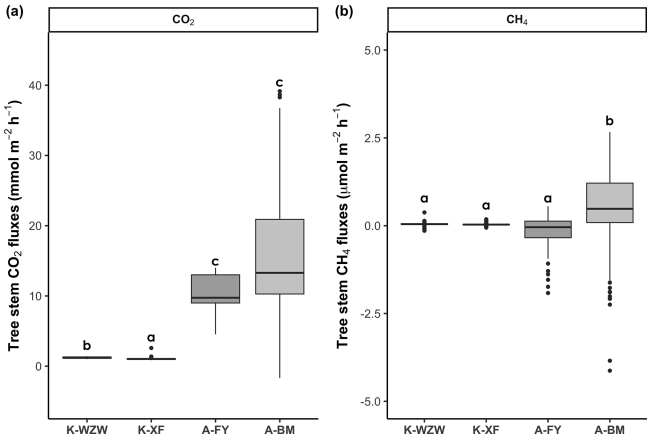

Figure 2. Differences in stem **(a)** CO_2 and **(b)** CH_4 fluxes among sites. Each data point represents a flux measurement taken during the tidal cycle, with 88 replicates for K-WZW, 82 replicates for K-XF, 75 replicates for A-FY, and 152 replicates for A-BM. The different letters above the boxplots indicate significant differences among sites, as determined by the Kruskal–Wallis test and Dunn's test ($p < 0.05$).

cycle, the CO_2 fluxes from the mangrove tree stems exhibited different trends across all sampling sites (Fig. 3). The emissions remained relatively constant during the tidal cycle, ranging from 1.01 to 1.43 mmol m^{-2} h^{-1} and from 0.85 to 2.59 mmol m^{-2} h^{-1} at the K-WZW and K-XF sites, respectively (Fig. 3a). However, a sharp emission peak (2.59 mmol m^{-2} h^{-1}) was observed at the K-XF site on day 2, when the tide was falling; this peak was 3-fold higher than the lowest flux (0.85 mmol m^{-2} h^{-1}) measured on the same day (Fig. 3a). The CO_2 flux at the A-FY and A-BM sites generally showed an increasing trend throughout the tidal cycle, ranging from 4.54 to 14.00 mmol m^{-2} h^{-1} and from −1.68 to 39.15 mmol m^{-2} h^{-1}, respectively (Fig. 3a). However, this trend was observed at the A-FY site only on day 1, when there was a distinct temporal trend in the increase in CO_2 flux relative to that at the A-BM site. Specifically, the former started to increase before the flood current entered and stabilized after high tide, reaching a peak flux (10.36 mmol m^{-2} h^{-1}) at the end of the measurement. Conversely, the latter showed no significant change during the rising tide, followed by a steep rise toward high tide and a slight decrease during the falling tide; however, the CO_2 flux still remained higher than that during the pre-flood tide, ranging from −1.68 to 33.24 mmol m^{-2} h^{-1} during the rising tide and from 8.74 to 39.15 mmol m^{-2} h^{-1} during the falling tide (Fig. 3a).

The CO_2 flux pattern observed during the tidal cycle differed between the tree stems and soils. Generally, the soil CO_2 flux peaked before and after high tide at all sites, during either the rising tide or the falling tide, when the flood current was just entering or leaving the sampling site (Fig. 3b).

Similar to the CO_2 fluxes, the CH_4 fluxes in *K. obovata* and *A. marina* exhibited distinct temporal trends during the tidal cycle (Fig. 4). In the *K. obovata* mangroves, there was significant variation in the stem CH_4 flux during the tidal cycle, ranging from −0.14 to 0.38 µmol m^{-2} h^{-1} and from −0.05 to 0.18 µmol m^{-2} h^{-1} at the K-WZW and K-XF sites, respectively, while consistent patterns were lacking between the sampling campaigns (Fig. 4a). The stem CH_4 flux of *A. marina* increased throughout the tidal cycle, ranging from −1.92 to 0.55 µmol m^{-2} h^{-1} and from −4.13 to 2.67 µmol m^{-2} h^{-1} at the A-FY and A-BM sites, respectively. Specifically, the tree stems of *A. marina* functioned as CH_4 sinks before tidal inundation (-0.53 ± 0.73 µmol m^{-2} h^{-1} at the A-FY site and -0.64 ± 1.51 µmol m^{-2} h^{-1} at the A-BM site), but the CH_4 flux gradually increased thereafter, eventually becoming a CH_4 source during low tide (0.18 ± 0.24 µmol m^{-2} h^{-1} at the A-FY site and 1.54 ± 0.56 µmol m^{-2} h^{-1} at the A-BM site). However, this pattern was not observed across all sampling campaigns (Fig. 4a).

For both mangrove species, the soil CH_4 flux during high tide (21.65 ± 45.29 µmol m^{-2} h^{-1}) was lower than that during low tide (47.70 ± 63.27 µmol m^{-2} h^{-1}) (Fig. 4b). Furthermore, there was a peak in the soil CH_4 flux during both tidal increases and decreases on all 3 sampling days, similar to that observed for the soil CO_2 flux (Figs. 3b; 4b).

During the tidal cycle, the CO_2 flux from the mangrove tree stems was positively correlated with the CH_4 flux during both the rising and falling tides. However, a significant relationship was detected only for *A. marina* (Fig. 5a; $p < 0.001$). The CO_2 and CH_4 fluxes from both the stems and soils were simultaneously measured, and a negative correlation between the stem and soil fluxes was observed across the two mangrove species. However, a significant relationship was detected only for *A. marina* during the falling tide (Fig. 5b, c; $p < 0.001$).

Since the tides at the sample sites were mainly semidiurnal tides, the average inundation time per day was calculated by multiplying the average time of high tide (when the water level was higher than 0 cm) during each sampling event by 2. The A-BM site exhibited the longest inundation time (15.33 h), while the inundation time during the sampling campaign was 6.69 h at the K-WZW and K-XF sites and 5.19 h at the A-FY site. The average highest tidal height (determined by the distance between the soil and water surface during high tide) was 58.1 cm at the K-WZW site, 70.5 cm at the K-XF site, 47.3 cm at the A-FY site, and 77.5 cm at the A-BM site. Different upscaling methods were applied to determine the tidal influence on the diurnal variation in the fluxes, where F_{BothTide} denotes the sum of the average fluxes during low and high tides, each multiplied by the corresponding time length, and F_{LowTide} denotes the average flux during low tides multiplied by 24 h. The GHG fluxes exhibited notable differences when tidal influences were considered (Table 1). Based on our findings, sampling only during low tide

Table 1. Comparison of upscaling methods with and without considering tidal influences on CO_2 and CH_4 fluxes in mangroves.

		K-WZW	K-XF	A-FY	A-BM
Dominant mangrove species		*Kandelia obovata*	*Kandelia obovata*	*Avicennia marina*	*Avicennia marina*
Sampling date		14–16 Jul 2022	15–17 Jun 2022	1–2 and 18 Jun 2022	27–29 Jul 2022
Sampling time (GMT+8)		08:00–15:00	08:30–15:00	10:00–16:30	04:30–15:00
Mean inundation time (h)		6.69	6.69	5.19	15.33
Mean highest tidal height (cm)		58.1	70.5	47.3	77.5
Flux measurement number (n)		88	82	75	152
Stem CO_2 flux ($\mathrm{mmol\,m^{-2}\,d^{-1}}$)	F_{BothTide}[a]	28.93	25.02	248.88	371.95
	F_{LowTide}[b]	28.94	24.82	245.95	339.99
	Difference (%)	0.03	0.81	1.19	9.40
Stem CH_4 flux ($\mathrm{\mu mol\,m^{-2}\,d^{-1}}$)	F_{BothTide}	1.18	0.81	−5.04	8.17
	F_{LowTide}	1.22	0.76	−5.49	−0.74
	Difference (%)	3.68	6.21	8.35	1200.25
Mean soil CO_2 flux ($\mathrm{mmol\,m^{-2}\,d^{-1}}$)		27.26	57.13	134.19	57.09
Mean soil CH_4 flux ($\mathrm{\mu mol\,m^{-2}\,d^{-1}}$)		149.77	217.42	2404.28	345.37
Mangrove forest area (ha)[c]		10.6	8.12	35.7	75.3
Mean tree height (m)[c]		4.0	5.1	1.8	3.2
Mean tree density ($\mathrm{tree\,m^{-2}}$)[c]		1.3	2.4	1.0	0.6
Mean diameter at breast height (cm)[c]		7.0	5.6	10.5	6.2
Stem lenticel density ($\mathrm{lenticels\,cm^{-2}}$)		0.08	0.05	1.83	2.96

[a] For F_{BothTide}, the average fluxes during low and high tides were added after being multiplied by the corresponding time length. [b] For F_{LowTide}, the average fluxes during low tides were multiplied by 24 h. The sampling date and time are provided in ISO 8601 format. [c] The data were derived from Lin et al. (2021).

may underestimate the stem CO_2 and CH_4 fluxes on a diurnal scale, except at the K-WZW site, where the stem CO_2 and CH_4 fluxes were 0.03 % and 3.68 % lower when considering tidal influences (Table 1). At the K-XF, A-FY, and A-BM sites, the differences in the stem CO_2 fluxes between the upscaling methods were smaller than the differences in the stem CH_4 fluxes, ranging from 0.81 % to 9.40 % (Table 1). The stem CH_4 fluxes at the K-XF site were approximately 6 % higher when considering tidal influences, as opposed to when tidal influences were ignored (Table 1). If the tidal influences were not accounted for, the mangrove tree stems at the A-FY and A-BM sites both acted as net CH_4 sinks, while the CH_4 sink capacity was 8 % and 1200 % lower, respectively, after accounting for tidal influences, resulting in the mangrove tree stem at the A-BM site turning into a net CH_4 source (Table 1).

4 Discussion

This study revealed distinct spatial and temporal variations in the CO_2 and CH_4 fluxes originating from tree stems and soils. Specifically, the sites dominated by *A. marina* exhibited CO_2 fluxes up to 15 times higher than those at the sites dominated by *K. obovata*. The tree stems of *A. marina* at the A-FY site acted as a net CH_4 sink, while the A-BM site emitted CH_4 at a rate approximately 3 times higher. In contrast, the tree stems of *K. obovata* at the K-WZW and K-XF sites were weak CH_4 sources compared to the tree stems at the A-BM site. The temporal dynamics during the tidal cycle also differed between the two mangrove species. Regarding *K. obovata*, the stem CO_2 and CH_4 fluxes at the K-WZW and K-XF sites lacked a consistent pattern between the sampling campaigns. In contrast, *A. marina* exhibited an increasing trend in CO_2 flux throughout the tidal cycle, whereas the CH_4 flux exhibited high temporal variability, functioning as

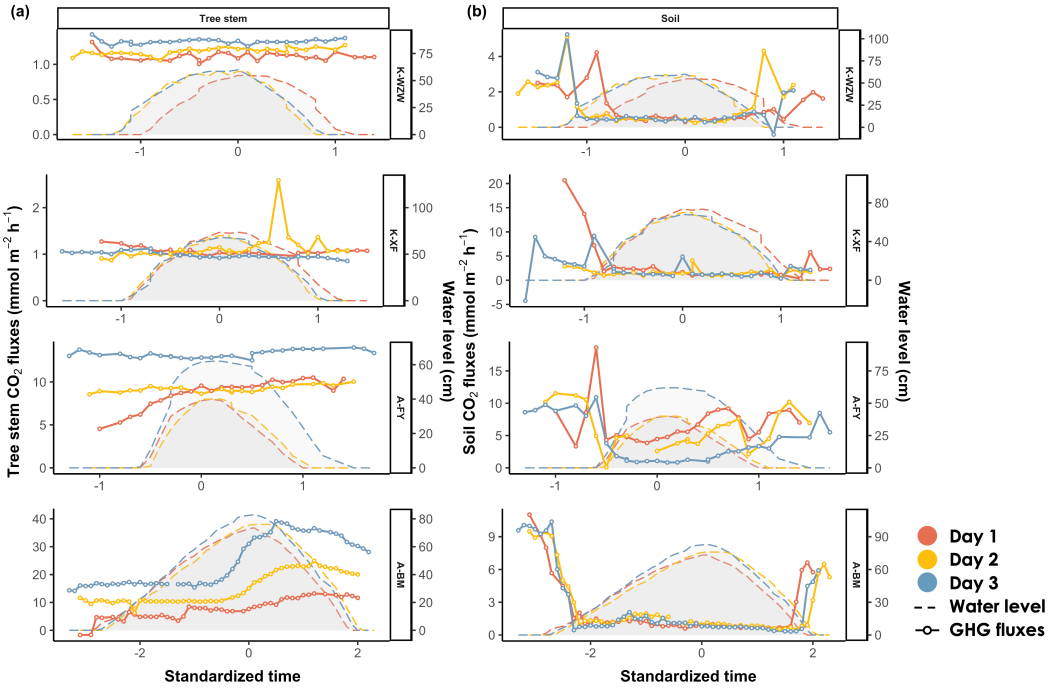

Figure 3. Variations in **(a)** stem CO_2 fluxes and **(b)** soil CO_2 fluxes during the tidal cycle. Time was standardized based on the time of the highest water level during the high-tide period (set as 0) and then adjusted by decrementing the time by 0.1 for every 10 min interval prior to the peak and incrementing the time by 0.1 for every 10 min interval after the peak. The average values of the flux and water level were calculated for each standardized time interval. The shaded area denotes the water level at the sampled tree. On days 1, 2, and 3, the plant data were arranged chronologically according to the sampling date.

a sink before tidal inundation and becoming a source during low tide at both the A-FY and A-BM sites. Therefore, our results suggest that different mangrove species – in this case, *K. obovata* and *A. marina* – may have varying capacities for CO_2 and CH_4 exchange with the atmosphere through tree stems during tidal cycles. Further investigation with a larger sample size is needed to examine the hypothesis of mangrove species variation in GHG fluxes.

In terms of biological factors, *A. marina* contains pneumatophores, while *K. obovata* does not. Pneumatophores may facilitate the transport of oxygen to the rhizosphere and increase the oxidation-reduction potential, thereby inhibiting the methanogenesis process (Dušek et al., 2021). However, they can also serve as pathways for deep-soil-layer CH_4 emissions, facilitating CH_4 transport (He et al., 2019; Lin et al., 2021). In this study, pneumatophores were not intentionally avoided during the measurements. Therefore, the presence of pneumatophores may contribute to the increased soil CH_4 flux in the *A. marina* mangrove forest.

GHG emissions from stems, whether originating from the soil or the stems themselves, require radial diffusion through the bark or lenticel to reach the atmosphere (Barba et al., 2019a). Radial diffusion is primarily influenced by biological factors, such as wood density, wood moisture content, and lenticel density (Covey and Megonigal, 2019). A higher lenticel density, in particular, creates more pathways for GHG emissions, resulting in increased emissions (Zhang et al., 2022). Based on visual observations in situ, we found that the tree stems at the A-FY and A-BM sites exhibited a significantly higher lenticel density than those at the K-WZW and K-XF sites (Table 1). Therefore, it is speculated that the higher lenticel density of *A. marina* facilitates the emission of GHGs from stems, resulting in a higher stem GHG flux at the A-FY and A-BM sites.

Previous studies on GHG emissions originating from mangrove tree stems were mostly conducted during low tide and under daylight conditions. Gao et al. (2021) showed that the stems of *Kandelia obovata* can both absorb and release CH_4, with average fluxes of -5.69 and $1.84\,\mu mol\,m^{-2}\,h^{-1}$, respectively. Zhang et al. (2022) reported higher CH_4 emissions from *K. obovata* stems ($7.04\,\mu mol\,m^{-2}\,h^{-1}$), which dominated the ecosystem's CH_4 flux in mangroves without pneumatophores. These results contradict the findings of this study, in which the CH_4 emissions of *K. obovata* stems contributed less than the soil emissions. Liao et al. (2024) measured lower stem CH_4 fluxes from *K. obovata* during winter ($0.54\,\mu mol\,m^{-2}\,h^{-1}$); these fluxes were 10 times higher than the average fluxes observed in this study. In the case of *A. marina*, the average stem CH_4 fluxes were $1.56\,\mu mol\,m^{-2}\,h^{-1}$ (Jeffrey

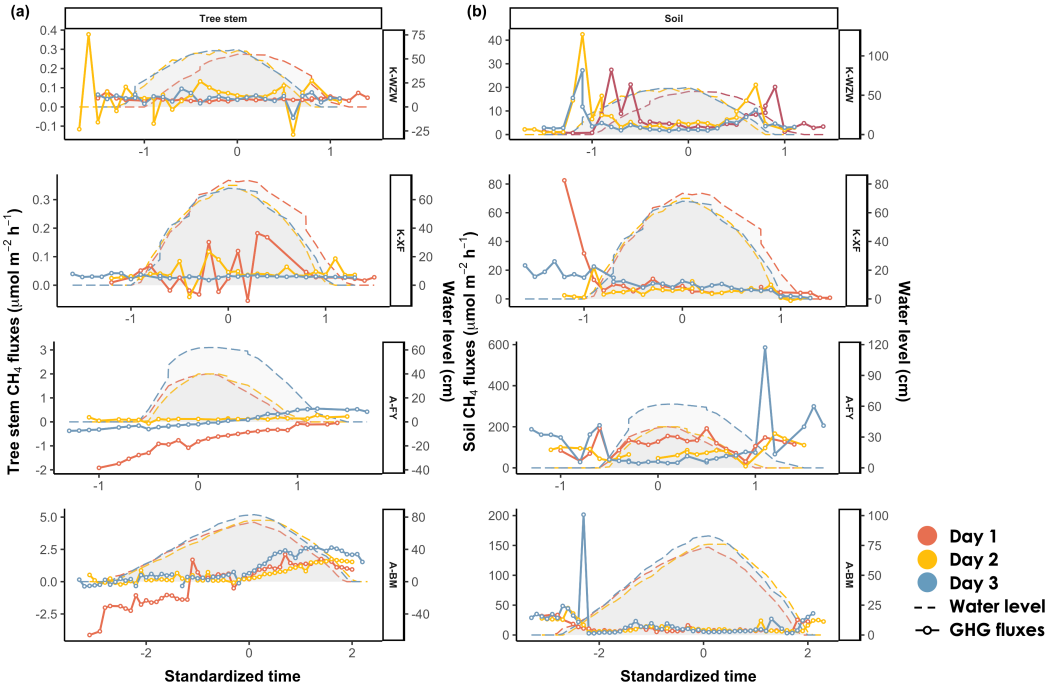

Figure 4. Variations in **(a)** stem CH_4 fluxes and **(b)** soil CH_4 fluxes during the tidal cycle. Time was standardized based on the time of the highest water level during the high-tide period (set as 0) and then adjusted by decrementing the time by 0.1 for every 10 min interval prior to the peak and incrementing the time by 0.1 for every 10 min interval after the peak. The average values of the flux and water level were calculated for each standardized time interval. The shaded area denotes the water level at the sampled tree. On days 1, 2, and 3, the plant data were chronologically arranged according to the sampling date.

et al., 2019) and 2.79 $\mu mol\,m^{-2}\,h^{-1}$ (Zhang et al., 2022) at mangrove sites located in Australia and China, respectively. The tree stems of *A. marina* also exhibited CH_4 consumption capacity, with fluxes ranging from −33.96 to 48.83 $\mu mol\,m^{-2}\,h^{-1}$, as reported in Gao et al. (2021). Regarding other mangrove species, *Kandelia candel* exhibited a stem CH_4 flux of $-1.81\,\mu mol\,m^{-2}\,h^{-1}$, while *Sonneratia apetala*, *Laguncularia racemosa*, and *Bruguiera* spp., all of which have the same specialized root structure as *A. marina*, exhibited stem CH_4 fluxes of 2.62, 0.87, and $-0.49\,\mu mol\,m^{-2}\,h^{-1}$, respectively (He et al., 2019). Epron et al. (2023) measured the CH_4 flux of the stems of *Bruguiera gymnorrhiza* throughout a 24 h cycle, with fluxes ranging from −0.36 to 263.16 $\mu mol\,m^{-2}\,h^{-1}$. In this study, the CH_4 fluxes in the stems of *A. marina* and *K. obovata* ranged from −0.14 to 0.38 $\mu mol\,m^{-2}\,h^{-1}$ ($0.05 \pm 0.06\,\mu mol\,m^{-2}\,h^{-1}$ at the K-WZW site and $0.04 \pm 0.04\,\mu mol\,m^{-2}\,h^{-1}$ at the K-XF site) and from −4.13 to 2.67 $\mu mol\,m^{-2}\,h^{-1}$ ($-0.17 \pm 0.52\,\mu mol\,m^{-2}\,h^{-1}$ at the A-FY site and $0.48 \pm 1.17\,\mu mol\,m^{-2}\,h^{-1}$ at the A-BM site), respectively; these values are at the low end of the reported range of stem CH_4 fluxes from previous studies (Table 2). Although CH_4 fluxes from mangrove tree stems generally decreased with increasing height (Epron et al., 2023; Gao et al., 2021; Jeffrey et al., 2019; Liao et al., 2024), average stem CH_4 fluxes in *A. marina* and *K. obovata* at similar heights to those in this study (> 1 m) were still higher. This may be due to site-specific variations in environmental conditions, tree physiology, and microbial activity, all of which can influence the production and consumption of methane by mangrove trees (Barba et al., 2019a; Covey and Megonigal, 2019). Further research is needed to delve into the underlying mechanisms, which were not fully elucidated in this study due to limited data availability.

The tree stem CO_2 and CH_4 fluxes exhibited similar temporal patterns during the tidal cycle. A significant positive relationship was also found between these fluxes, indicating that CO_2 and CH_4 emitted by mangrove tree stems may originate from the same source or be influenced by the same mechanism during the tidal cycle (Liao et al., 2024). According to previous studies, CO_2 emissions primarily occur through root respiration and stem respiration, as well as via internal plant metabolism and transport from soils (Teskey et al., 2008). In contrast, CH_4 may be emitted or absorbed by methanogens and methanotrophs present in tree bark or heartwood (Feng et al., 2022; Jeffrey et al., 2021). CH_4 emitted by tree stems may also originate from the soil, where CH_4 produced in the soil enters the root system, moves into the tree's aerenchyma tissues or xylem, and is subsequently directly released into the atmosphere through lenticels or tree

Table 2. Comparison of stem methane (CH_4) fluxes in mangrove ecosystems reported in this study with previous literature. The values are presented as the range (the minimum value to maximum value) and/or the mean ± standard deviation (given in parentheses).

Site	Period	Species	Height (m)	Stem CH_4 fluxes ($\mu mol\ m^{-2}\ h^{-1}$)	Measurement technique	Reference
Australia	Winter (Aug 2018)	*A. marina*	0.12	0.01 to 21.00 (4.03 ± 1.15)	CRDS	Jeffrey et al. (2019)
			0.4	0.03 to 6.84 (1.21 ± 0.30)		
			0.8	0.31 to 4.77 (1.25 ± 0.19)		
			1.51	0.51 to 2.62 (1.14 ± 0.10)		
China	All seasons (Feb 2012–Nov 2013)	*L. racemosa*	ND	(0.87 ± 0.81)	GC	He et al. (2019)
		S. apetala		(2.61 ± 1.25)		
		K. candel		(−1.81 ± 1.00)		
		B. gymnorrhiza *B. sexangula*		(−0.49 ± 0.75)		
	Summer (Jul 2019–Aug 2019)	*K. obovata* (site 1)	0.4	−78.78 to 11.35 (−7.12)	CRDS	Gao et al. (2021)
			1.4	−52.67 to 8.89 (−4.39)		
		K. obovata (site 2)	0.4	−32.36 to 26.90 (2.97)		
			1.4	−9.95 to 51.38 (1.63)		
		A. marina	0.4	−33.96 to 22.50		
			1.4	−23.34 to 48.83		
		Aegiceras corniculatum	0.4	−131.19 to 225.16		
			1.4	−41.42 to 42.43		
	Winter (Jan 2018) Summer (Jul 2018)	*K. obovata*	0–1.25	(7.04 ± 3.96)	GC	Zhang et al. (2022)
		A. corniculatum		(5.42 ± 3.04)		
		A. marina		(2.79 ± 2.13)		
	Winter (Dec 2021–Mar 2021)	*K. obovata*	0.7	(0.68 ± 0.17)		Liao et al. (2024)
			1.2	(0.57 ± 0.19)		
			1.7	(0.37 ± 0.13)		
		S. apetala	0.7	(1.25 ± 0.21)		
			1.2	(0.84 ± 0.14)		
			1.7	(0.42 ± 0.12)		
Japan	Summer (Jul 2022)	*B. gymnorrhiza*	0.3	1.80 to 825.12 (143.64)	CEAS	Epron et al. (2023)
			0.6–1.5	−0.36 to 263.16 (30.6)		
Taiwan	Summer (Jun 2022–Jul 2022)	*K. obovata* (K-WZW)	1.1	−0.14 to 0.38 (0.05 ± 0.06)		This study
		K. obovata (K-XF)		−0.05 to 0.18 (0.04 ± 0.04)		
		A. marina (A-FY)		−1.92 to 0.55 (−0.17 ± 0.52)		
		A. marina (A-BM)		−4.13 to 2.67 (0.48 ± 1.17)		

GC stands for gas chromatography, CRDS for cavity ring-down spectroscopy, CEAS for cavity-enhanced absorption spectroscopy, and ND for no data.

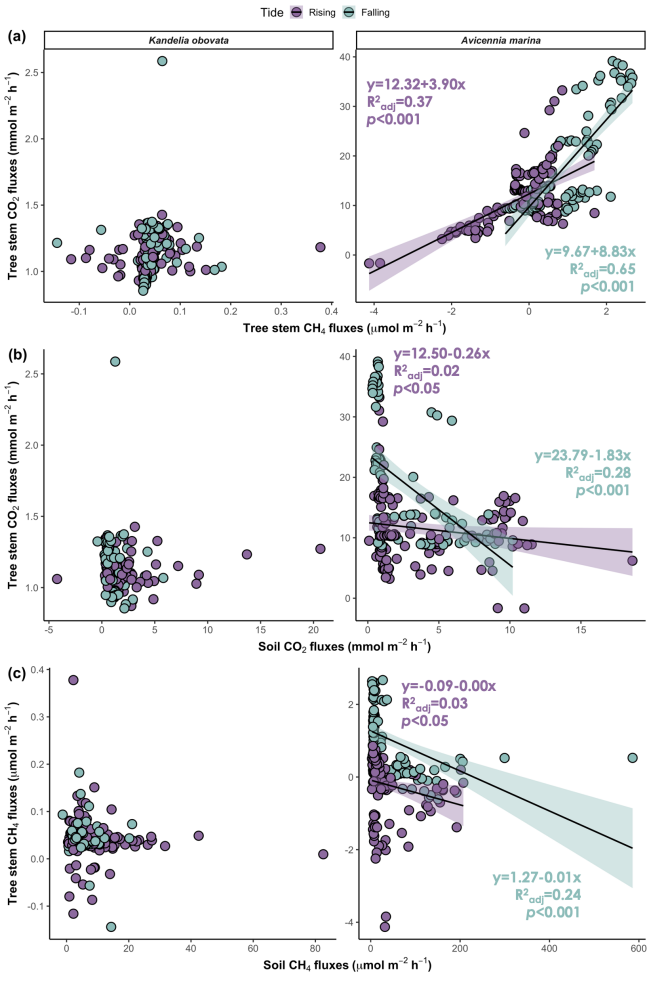

Figure 5. Relationships between **(a)** stem CO_2 fluxes and CH_4 fluxes, **(b)** stem CO_2 fluxes and soil CO_2 fluxes, and **(c)** stem CH_4 fluxes and soil CH_4 fluxes. The shaded areas denote the 95 % confidence intervals of the regression lines. R^2_{adj}: adjusted R^2.

stems (Barba et al., 2019a; Covey and Megonigal, 2019). Therefore, the fixation of CO_2, oxidation of CH_4, and emission of both GHGs by the tree stem may originate from the tree stem itself or from the soil. In this study, the transformation of tree stems from CH_4 sinks to CH_4 sources was observed in the *A. marina* mangrove forest. This observation indicates that CH_4 emitted by tree stems may be affected by different sources during different periods of the tidal cycle.

The transport mechanism of GHGs in the stem is similar to that in herbaceous plants, occurring mainly via diffusion or evaporation, either jointly or individually. The diffusion direction mainly depends on the CH_4 concentration gradient. For example, if the gas concentration in the rhizosphere is high, GHGs can enter the plant root system in either gaseous form or liquid form, thus entering the aerenchyma or xylem tissue (Vroom et al., 2022). Aerenchyma is a specialized tissue found in many mangrove tree species (Evans, 2004). It comprises air-filled spaces that create gas transport pathways within the plant. Aerenchyma facilitates gas movement, including that of CO_2 and CH_4, within stems. Within the aerenchyma, CO_2 and CH_4 can diffuse or passively flow along concentration gradients. This transport pathway allows gases to move vertically within the plant – from the roots, through the stem, and ultimately into the atmosphere. Aerenchyma tissue is particularly important for CH_4 transport because CH_4 is produced in oxygen-limited soils or in the rhizosphere by methanogens. The aerenchyma provides a direct pathway for CH_4 to move upward through the stems and be emitted into the atmosphere (Yáñez-Espinosa and Angeles, 2022). CO_2 and CH_4 can also dissolve during dilution and be transported within the xylem via sap flux (Takahashi et al., 2022). This study revealed the transition of mangrove tree stems from CH_4 sinks to CH_4 sources within the tidal cycle, a phenomenon that has not been observed in other studies, even with high-frequency measurements of upland tree stems at 1 h intervals (Barba et al., 2019b). We speculate that tree stems of *A. marina* may absorb CH_4 through the presence of methanotrophs during low tide (Jeffrey et al., 2021). During inundation, the diffusion of CH_4 produced in the deep soil layer may be restricted by water pressure (Tong et al., 2013) since the pore spaces are filled with water. Tong et al. (2010) also reported a significantly lower CH_4 flux during inundation than during low tide. Therefore, we hypothesize that CH_4 produced in the soil during inundation periods may be primarily emitted into the atmosphere through tree stems (Vroom et al., 2022; Yáñez-Espinosa and Angeles, 2022) rather than across the water–atmosphere interface via diffusion or ebullition (Li et al., 2021), resulting in the observed gradual increase in CH_4 flux throughout the tidal cycle. This hypothesis is also supported by the negative relationship between the soil and stem CH_4 fluxes in *A. marina* observed during both rising and falling tides in this study. However, the CH_4 flux in the tree stems of *Bruguiera gymnorrhiza* peaked after the tide receded (Epron et al., 2023), which does not support this hypothesis. It is critical to note that the specific mechanisms driving the observed peaks may vary depending on factors such as mangrove species, environmental conditions, tidal dynamics, and site-specific characteristics. However, further research is necessary to fully comprehend the underlying mechanisms.

To our knowledge, this study is the first to simultaneously measure CH_4 fluxes in both stems and soils throughout the tidal cycle, even during tidal inundation. When quantifying the GHG emissions of mangrove tree stems, discrete and continuous methods are two common measurement approaches. Discrete measurements involve sampling at specific time points with a lower temporal resolution and are practical and cost-effective. Continuous measurements provide real-time monitoring with a high temporal resolution, accurately capturing short-term fluctuations and peak emissions, but require specialized equipment and technical expertise. When considering tidal influences through continu-

ous measurements, CH_4 emitted by mangrove tree stems was significantly higher, with differences of up to 1200 % in the stem CH_4 fluxes. Conversely, the upscaled CH_4 flux accounting for tides in tidal salt marshes was lower (Huang et al., 2019). When quantifying the GHG emissions of mangrove tree stems, discrete measurements are commonly used due to sampling difficulty at night and during high tide. Although discrete measurements can still provide reliable estimates of the average emission rate over a specific period, they are useful only for broader-scale quantification and for carbon and CH_4 budgeting models. This study highlights the need for continuous measurements of GHG fluxes in coastal ecosystems, which can provide a more detailed understanding of emission patterns, aid in overall emission quantification, help individuals identify key drivers and mechanisms, reduce uncertainty in GHG emissions, and facilitate the assessment of the impacts of specific events or environmental variables (Capooci and Vargas, 2022). However, in contrast to practical, feasible, and cost-effective discrete measurements, continuous measurements require specialized equipment, technical expertise, and intensive labor. It should also be noted that considerable differences were mainly observed at the A-BM site, which had the longest inundation time and the highest water table.

This study provides insights into the potential tidal influence on GHG fluxes from mangrove tree stems. However, several uncertainties require further investigation. First, the study was conducted during summer and daylight hours, which may have resulted in higher fluxes due to the effects of higher temperatures and the sap-flux-dependent transport mechanism within the tree stems (Barba et al., 2019b; Köhn et al., 2021; Pangala et al., 2015; Pitz et al., 2018; Takahashi et al., 2022; Wang et al., 2016; Zhang et al., 2022). Second, the sampling campaign was conducted during the spring tide, and CH_4 fluxes in tidal wetlands may differ between spring and neap tides (Huang et al., 2019; Tong et al., 2013). Third, sampling only at a height of 110 cm may have resulted in height-related GHG flux variations within mangrove tree stems being overlooked, as observed in other studies (Epron et al., 2023; Jeffrey et al., 2019; Moldaschl et al., 2021; Pangala et al., 2013, 2014, 2015; Sjögersten et al., 2020). Finally, with the limited data availability, it is still uncertain whether there is a significant difference in GHG emissions from tree stems between the two mangrove species.

5 Conclusion

This study revealed distinct temporal variations in CO_2 and CH_4 fluxes in the tree stems of *A. marina* and *K. obovata* throughout tidal cycles. While GHG fluxes in *K. obovata* stems displayed inconsistent patterns, CH_4 fluxes in *A. marina* stems suggested a transition in the stems from being a sink to a source, indicating the influence of different sources and mechanisms during different tidal phases. When considering tidal influences, the stem CH_4 flux in *A. marina* may vary by up to 1200 %, causing the stem to transition from a net CH_4 sink to a source. This study highlights the need to consider tidal influences and species when quantifying GHG fluxes in mangrove tree stems and the potential limitations of discrete measurements relative to continuous measurements. However, further study is needed to fully understand the underlying mechanisms driving the observed flux variations and to improve our understanding of, and reduce uncertainty in, GHG dynamics in mangrove ecosystems.

Data availability. The original contributions presented in the study are included in Sect. 3. We encourage prospective data users to contact us before embarking on any analysis.

Supplement. The supplement related to this article is available online at: https://doi.org/10.5194/bg-21-5247-2024-supplement.

Author contributions. ZJY: methodology, investigation, visualization, and writing (original draft). WJL: methodology, investigation, and visualization. CWL: methodology, investigation, and visualization. HJL: conceptualization, supervision, writing (review and editing), and funding acquisition.

Competing interests. The contact author has declared that none of the authors has any competing interests.

Disclaimer. Publisher's note: Copernicus Publications remains neutral with regard to jurisdictional claims made in the text, published maps, institutional affiliations, or any other geographical representation in this paper. While Copernicus Publications makes every effort to include appropriate place names, the final responsibility lies with the authors.

Acknowledgements. This study was supported by the Innovation and Development Center of Sustainable Agriculture via the Featured Areas Research Center Program within the framework of the Higher Education Sprout Project hosted by the Ministry of Education (MOE) of Taiwan.

Financial support. This research was supported by the Ministry of Science and Technology of Taiwan (grant no. 112-2621-M-005-004).

Review statement. This paper was edited by Gwenaël Abril and reviewed by two anonymous referees.

References

Bahlmann, E., Weinberg, I., Lavrič, J. V., Eckhardt, T., Michaelis, W., Santos, R., and Seifert, R.: Tidal controls on trace gas dynamics in a seagrass meadow of the Ria Formosa lagoon (southern Portugal), Biogeosciences, 12, 1683–1696, https://doi.org/10.5194/bg-12-1683-2015, 2015.

Barba, J., Poyatos, R., and Vargas, R.: Automated measurements of greenhouse gases fluxes from tree stems and soils: Magnitudes, patterns and drivers, Sci. Rep., 9, 4005, https://doi.org/10.1038/s41598-019-39663-8, 2019a.

Barba, J., Bradford, M. A., Brewer, P. E., Bruhn, D., Covey, K., Haren, J., Megonigal, J. P., Mikkelsen, T. N., Pangala, S. R., Pihlatie, M., Poulter, B., Rivas-Ubach, A., Schadt, C. W., Terazawa, K., Warner, D. L., Zhang, Z., and Vargas, R.: Methane emissions from tree stems: A new frontier in the global carbon cycle, New Phytol., 222, 18–28, https://doi.org/10.1111/nph.15582, 2019b.

Billerbeck, M., Werner, U., Polerecky, L., Walpersdorf, E., deBeer, D., and Huettel, M.: Surficial and deep pore water circulation governs spatial and temporal scales of nutrient recycling in intertidal sand flat sediment, Mar. Ecol.-Prog. Ser., 326, 61–76, https://doi.org/10.3354/meps326061, 2006.

Carmichael, M. J., Bernhardt, E. S., Bräuer, S. L., and Smith, W. K.: The role of vegetation in methane flux to the atmosphere: Should vegetation be included as a distinct category in the global methane budget?, Biogeochemistry, 119, 1–24, https://doi.org/10.1007/s10533-014-9974-1, 2014.

Covey, K. R. and Megonigal, J. P.: Methane production and emissions in trees and forests, New Phytol., 222, 35–51, https://doi.org/10.1111/nph.15624, 2019.

Capooci, M. and Vargas, R.: Trace gas fluxes from tidal salt marsh soils: implications for carbon–sulfur biogeochemistry, Biogeosciences, 19, 4655–4670, https://doi.org/10.5194/bg-19-4655-2022, 2022.

Duarte de Paula Costa, M. and Macreadie, P. I.: The Evolution of Blue Carbon Science, Wetlands, 42, 109, https://doi.org/10.1007/s13157-022-01628-5, 2022.

Dušek, J., Nguyen, V. X., Le, T. X., and Pavelka, M.: Methane and carbon dioxide emissions from different ecosystems at the end of dry period in South Vietnam, Trop. Ecol., 62, 1–16, https://doi.org/10.1007/s42965-020-00118-1, 2021.

Epron, D., Mochidome, T., Bassar, A. T. M. Z., and Suwa, R.: Variability in methane emissions from stems and buttress roots of *Bruguiera Gymnorrhiza* trees in a subtropical mangrove forest, Ecol. Res., 1440–1703, https://doi.org/10.1111/1440-1703.12415, 2023.

Evans, D. E.: Aerenchyma formation, New Phytol., 161, 35–49, https://doi.org/10.1046/j.1469-8137.2003.00907.x, 2004.

Feng, H., Guo, J., Ma, X., Han, M., Kneeshaw, D., Sun, H., Malghani, S., Chen, H., and Wang, W.: Methane emissions may be driven by hydrogenotrophic methanogens inhabiting the stem tissues of poplar, New Phytol., 233, 182–193, https://doi.org/10.1111/nph.17778, 2022.

Gao, C.-H., Zhang, S., Ding, Q.-S., Wei, M.-Y., Li, H., Li, J., Wen, C., Gao, G.-F., Liu, Y., Zhou, J.-J., Zhang, J.-Y., You, Y.-P., and Zheng, H.-L.: Source or sink? A study on the methane flux from mangroves stems in Zhangjiang estuary, southeast coast of China, Sci. Total. Environ., 788, 147782, https://doi.org/10.1016/j.scitotenv.2021.147782, 2021.

Gauci, V., Gowing, D. J. G., Hornibrook, E. R. C., Davis, J. M., and Dise, N. B.: Woody stem methane emission in mature wetland alder trees, Atmos. Environ., 44, 2157–2160, https://doi.org/10.1016/j.atmosenv.2010.02.034, 2010.

He, Y., Guan, W., Xue, D., Liu, L., Peng, C., Liao, B., Hu, J., Zhu, Q., Yang, Y., Wang, X., Zhou, G., Wu, Z., and Chen, H.: Comparison of methane emissions among invasive and native mangrove species in Dongzhaigang, Hainan Island, Sci. Total. Environ., 697, 133945, https://doi.org/10.1016/j.scitotenv.2019.133945, 2019.

Huang, J., Jiafang Huang, Luo, M., Min Luo, Liu, Y., Yuxue, Z., and Tan, J.: Effects of Tidal Scenarios on the Methane Emission Dynamics in the Subtropical Tidal Marshes of the Min River Estuary in Southeast China, Int. J. Env. Res. Pub. He., 16, 2790, https://doi.org/10.3390/ijerph16152790, 2019.

Jackson, R. B., Saunois, M., Bousquet, P., Canadell, J. G., Poulter, B., Stavert, A. R., Bergamaschi, P., Niwa, Y., Segers, A., and Tsuruta, A.: Increasing anthropogenic methane emissions arise equally from agricultural and fossil fuel sources, Environ. Res. Lett., 15, 071002, https://doi.org/10.1088/1748-9326/ab9ed2, 2020.

Jeffrey, L. C., Reithmaier, G., Sippo, J. Z., Johnston, S. G., Tait, D. R., Harada, Y., and Maher, D. T.: Are methane emissions from mangrove stems a cryptic carbon loss pathway? Insights from a catastrophic forest mortality, New Phytol., 224, 146–154, https://doi.org/10.1111/nph.15995, 2019.

Jeffrey, L. C., Maher, D. T., Chiri, E., Leung, P. M., Nauer, P. A., Arndt, S. K., Tait, D. R., Greening, C., and Johnston, S. G.: Bark-dwelling methanotrophic bacteria decrease methane emissions from trees, Nat. Commun., 12, 2127, https://doi.org/10.1038/s41467-021-22333-7, 2021.

Jeffrey, L. C., Moras, C. A., Tait, D. R., Johnston, S. G., Call, M., Sippo, J. Z., Jeffrey, N. C., Laicher-Edwards, D., and Maher, D. T.: Large Methane Emissions From Tree Stems Complicate the Wetland Methane Budget, J. Geophys. Res.-Biogeo., 128, e2023JG007679, https://doi.org/10.1029/2023JG007679, 2023.

Jeffrey, L. C., Johnston, S. G., Tait, D. R., Dittmann, J., and Maher, D. T.: Rapid bark-mediated tree stem methane transport occurs independently of the transpiration stream in *Melaleuca quinquenervia*, New Phytol., 242, 49–60, https://doi.org/10.1111/nph.19404, 2024.

Köhn, D., Günther, A., Schwabe, I., and Jurasinski, G.: Short-lived peaks of stem methane emissions from mature black alder (*Alnus Glutinosa* (L.) Gaertn.) – Irrelevant for ecosystem methane budgets?, Plant-Environ. Interact., 2, 16–27, https://doi.org/10.1002/pei3.10037, 2021.

Kutschera, E., Khalil, A., Rice, A., and Rosenstiel, T.: Mechanisms of methane transport through *Populus trichocarpa*, Biogeosciences Discuss. [preprint], https://doi.org/10.5194/bg-2016-60, in review, 2016.

Lee, L.-H., Hsieh, L.-Y., and Lin, H.-J.: In situ production and respiration of the benthic community during emersion on subtropical intertidal sandflats, Mar. Ecol.-Prog. Ser., 441, 33–47, https://doi.org/10.3354/meps09362, 2011.

Lenhart, K., Weber, B., Elbert, W., Steinkamp, J., Clough, T., Crutzen, P., Pöschl, U., and Keppler, F.: Nitrous oxide and methane emissions from cryptogamic covers, Glob. Change Biol., 21, 3889–3900, https://doi.org/10.1111/gcb.12995, 2015.

Liao, X., Wang, Y., Malghani, S., Zhu, X., Cai, W., Qin, Z., and Wang, F.: Methane and nitrous oxide emissions and related microbial communities from mangrove stems on Qi'ao Island, Pearl River Estuary in China, Sci. Total. Environ., 915, 170062, https://doi.org/10.1016/j.scitotenv.2024.170062, 2024.

Li, S., Chen, P., Huang, J., Hsueh, M., Hsieh, L., Lee, C., and Lin, H.: Factors regulating carbon sinks in mangrove ecosystems, Glob. Change Biol., 24, 4195–4210, https://doi.org/10.1111/gcb.14322, 2018.

Li, Y., Wang, D., Chen, Z., Chen, J., Hu, H., and Wang, R.: Methane Emissions during the Tide Cycle of a Yangtze Estuary Salt Marsh, Atmosphere, 12, 245, https://doi.org/10.3390/atmos12020245, 2021.

Lin, C.-W., Kao, Y.-C., Chou, M.-C., Wu, H.-H., Ho, C.-W., and Lin, H.-J.: Methane Emissions from Subtropical and Tropical Mangrove Ecosystems in Taiwan, Forests, 11, 470, https://doi.org/10.3390/f11040470, 2020.

Lin, C.-W., Kao, Y.-C., Lin, W.-J., Ho, C.-W., and Lin, H.-J.: Effects of Pneumatophore Density on Methane Emissions in Mangroves, Forests, 12, 314, https://doi.org/10.3390/f12030314, 2021.

Lin, C.-W., Lin, W.-J., Ho, C.-W., Kao, Y.-C., Yong, Z.-J., and Lin, H.-J.: Flushing emissions of methane and carbon dioxide from mangrove soils during tidal cycles, Sci. Total Environ., 919, 170768, https://doi.org/10.1016/j.scitotenv.2024.170768, 2024.

Lin, W.-J., Lin, C.-W., Wu, H.-H., Kao, Y.-C., and Lin, H.-J.: Mangrove carbon budgets suggest the estimation of net production and carbon burial by quantifying litterfall, CATENA, 232, 107421, https://doi.org/10.1016/j.catena.2023.107421, 2023.

Machacova, K., Borak, L., Agyei, T., Schindler, T., Soosaar, K., Mander, Ü., and Ah-Peng, C.: Trees as net sinks for methane (CH_4) and nitrous oxide (N_2O) in the lowland tropical rain forest on volcanic Réunion Island, New Phytol., 229, 1983–1994, https://doi.org/10.1111/nph.17002, 2021.

Moldaschl, E., Kitzler, B., Machacova, K., Schindler, T., and Schindlbacher, A.: Stem CH_4 and N_2O fluxes of *Fraxinus excelsior* and *Populus alba* trees along a flooding gradient, Plant Soil, 461, 407–420, https://doi.org/10.1007/s11104-020-04818-4, 2021.

Peacock, M., Lawson, C., Gowing, D., and Gauci, V.: Water table depth and plant species determine the direction and magnitude of methane fluxes in floodplain meadow soils, Ecol. Evol., 14, e11147, https://doi.org/10.1002/ece3.11147, 2024.

Pangala, S. R., Moore, S., Hornibrook, E. R. C., and Gauci, V.: Trees are major conduits for methane egress from tropical forested wetlands, New Phytol., 197, 524–531, https://doi.org/10.1111/nph.12031, 2013.

Pangala, S. R., Gowing, D. J., Hornibrook, E. R. C., and Gauci, V.: Controls on methane emissions from *Alnus Glutinosa* saplings, New Phytol., 201, 887–896, https://doi.org/10.1111/nph.12561, 2014.

Pangala, S. R., Hornibrook, E. R. C., Gowing, D. J., and Gauci, V.: The contribution of trees to ecosystem methane emissions in a temperate forested wetland, Glob. Change Biol., 21, 2642–2654, https://doi.org/10.1111/gcb.12891, 2015.

Pangala, S. R., Enrich-Prast, A., Basso, L. S., Peixoto, R. B., Bastviken, D., Hornibrook, E. R. C., Gatti, L. V., Marotta, H., Calazans, L. S. B., Sakuragui, C. M., Bastos, W. R., Malm, O., Gloor, E., Miller, J. B., and Gauci, V.: Large emissions from floodplain trees close the Amazon methane budget, Nature, 552, 230–234, https://doi.org/10.1038/nature24639, 2017.

Pitz, S. L., Megonigal, J. P., Chang, C.-H., and Szlavecz, K.: Methane fluxes from tree stems and soils along a habitat gradient, Biogeochemistry, 137, 307–320, https://doi.org/10.1007/s10533-017-0400-3, 2018.

Rosentreter, J. A., Maher, D. T., Erler, D. V., Murray, R. H., and Eyre, B. D.: Methane emissions partially offset "blue carbon" burial in mangroves, Sci. Adv., 4, eaao4985, https://doi.org/10.1126/sciadv.aao4985, 2018.

Saunois, M., Stavert, A. R., Poulter, B., Bousquet, P., Canadell, J. G., Jackson, R. B., Raymond, P. A., Dlugokencky, E. J., Houweling, S., Patra, P. K., Ciais, P., Arora, V. K., Bastviken, D., Bergamaschi, P., Blake, D. R., Brailsford, G., Bruhwiler, L., Carlson, K. M., Carrol, M., Castaldi, S., Chandra, N., Crevoisier, C., Crill, P. M., Covey, K., Curry, C. L., Etiope, G., Frankenberg, C., Gedney, N., Hegglin, M. I., Höglund-Isaksson, L., Hugelius, G., Ishizawa, M., Ito, A., Janssens-Maenhout, G., Jensen, K. M., Joos, F., Kleinen, T., Krummel, P. B., Langenfelds, R. L., Laruelle, G. G., Liu, L., Machida, T., Maksyutov, S., McDonald, K. C., McNorton, J., Miller, P. A., Melton, J. R., Morino, I., Müller, J., Murguia-Flores, F., Naik, V., Niwa, Y., Noce, S., O'Doherty, S., Parker, R. J., Peng, C., Peng, S., Peters, G. P., Prigent, C., Prinn, R., Ramonet, M., Regnier, P., Riley, W. J., Rosentreter, J. A., Segers, A., Simpson, I. J., Shi, H., Smith, S. J., Steele, L. P., Thornton, B. F., Tian, H., Tohjima, Y., Tubiello, F. N., Tsuruta, A., Viovy, N., Voulgarakis, A., Weber, T. S., van Weele, M., van der Werf, G. R., Weiss, R. F., Worthy, D., Wunch, D., Yin, Y., Yoshida, Y., Zhang, W., Zhang, Z., Zhao, Y., Zheng, B., Zhu, Q., Zhu, Q., and Zhuang, Q.: The Global Methane Budget 2000–2017, Earth Syst. Sci. Data, 12, 1561–1623, https://doi.org/10.5194/essd-12-1561-2020, 2020.

Schindler, T., Mander, Ü., Machacova, K., Espenberg, M., Krasnov, D., Escuer-Gatius, J., Veber, G., Pärn, J., and Soosaar, K.: Short-term flooding increases CH_4 and N_2O emissions from trees in a riparian forest soil-stem continuum, Sci. Rep., 10, 3204, https://doi.org/10.1038/s41598-020-60058-7, 2020.

Schindler, T., Machacova, K., Mander, Ü., Escuer-Gatius, J., and Soosaar, K.: Diurnal Tree Stem CH_4 and N_2O Flux Dynamics from a Riparian Alder Forest, Forests, 12, 863, https://doi.org/10.3390/f12070863, 2021.

Siegenthaler, A., Welch, B., Pangala, S. R., Peacock, M., and Gauci, V.: Technical Note: Semi-rigid chambers for methane gas flux measurements on tree stems, Biogeosciences, 13, 1197–1207, https://doi.org/10.5194/bg-13-1197-2016, 2016.

Sjögersten, S., Siegenthaler, A., Lopez, O. R., Aplin, P., Turner, B., and Gauci, V.: Methane emissions from tree stems in neotropical peatlands, New Phytol., 225, 769–781, https://doi.org/10.1111/nph.16178, 2020.

Sturm, K., Werner, U., Grinham, A., and Yuan, Z.: Tidal variability in methane and nitrous oxide emissions along a subtropical estuarine gradient, Estuar. Coast. Shelf S., 192, 159–169, https://doi.org/10.1016/j.ecss.2017.04.027, 2017.

Takahashi, K., Sakabe, A., Azuma, W. A., Itoh, M., Imai, T., Matsumura, Y., Tateishi, M., and Kosugi, Y.: Insights into the mechanism of diurnal variations in methane emission from the stem surfaces of *Alnus Japonica*, New Phytol., 235, 1757–1766, https://doi.org/10.1111/nph.18283, 2022.

Terazawa, K., Ishizuka, S., Sakata, T., Yamada, K., and Takahashi, M.: Methane emissions from stems of Fraxinus mandshurica var. japonica trees in a floodplain forest, Soil Biol. Biochem., 39, 2689–2692, https://doi.org/10.1016/j.soilbio.2007.05.013, 2007.

Terazawa, K., Yamada, K., Ohno, Y., Sakata, T., and Ishizuka, S.: Spatial and temporal variability in methane emissions from tree stems of *Fraxinus mandshurica* in a cool-temperate floodplain forest, Biogeochemistry, 123, 349–362, https://doi.org/10.1007/s10533-015-0070-y, 2015.

Terazawa, K., Tokida, T., Sakata, T., Yamada, K., and Ishizuka, S.: Seasonal and weather-related controls on methane emissions from the stems of mature trees in a cool-temperate forested wetland, Biogeochemistry, 156, 211–230, https://doi.org/10.1007/s10533-021-00841-4, 2021.

Teskey, R. O., Saveyn, A., Steppe, K., and McGuire, M. A.: Origin, fate and significance of CO_2 in tree stems, New Phytol., 177, 17–32, https://doi.org/10.1111/j.1469-8137.2007.02286.x, 2008.

Tong, C., Wang, W.-Q., Zeng, C.-S., and Marrs, R.: Methane (CH_4) emission from a tidal marsh in the Min River estuary, southeast China, J. Environ. Sci. Health A, 45, 506–516, https://doi.org/10.1080/10934520903542261, 2010.

Tong, C., Tong, C., Huang, J. F., Hu, Z. Q., and Jin, Y. F.: Diurnal Variations of Carbon Dioxide, Methane, and Nitrous Oxide Vertical Fluxes in a Subtropical Estuarine Marsh on Neap and Spring Tide Days, Estuaries Coasts, 36, 633–642, https://doi.org/10.1007/s12237-013-9596-1, 2013.

Vroom, R. J. E., Van Den Berg, M., Pangala, S. R., Van Der Scheer, O. E., and Sorrell, B. K.: Physiological processes affecting methane transport by wetland vegetation – A review, Aquat. Bot., 182, 103547, https://doi.org/10.1016/j.aquabot.2022.103547, 2022.

Wang, Z., Gu, Q., Deng, F., Huang, J., Megonigal, J. P., Yu, Q., Lü, X., Li, L., Chang, S., Zhang, Y., Feng, J., and Han, X.: Methane emissions from the trunks of living trees on upland soils, New Phytol., 211, 429–439, https://doi.org/10.1111/nph.13909, 2016.

Yamamoto, A., Hirota, M., Suzuki, S., Oe, Y., Zhang, P., Mariko, S., and Mariko, S.: Effects of tidal fluctuations on CO_2 and CH_4 fluxes in the littoral zone of a brackish-water lake, Limnology, 10, 229–237, https://doi.org/10.1007/s10201-009-0284-6, 2009.

Yáñez-Espinosa, L. and Angeles, G.: Does mangrove stem bark have an internal pathway for gas flow?, Trees, 36, 361–377, https://doi.org/10.1007/s00468-021-02210-y, 2022.

Zhang, C., Zhang, Y., Luo, M., Tan, J., Chen, X., Tan, F., and Huang, J.: Massive methane emission from tree stems and pneumatophores in a subtropical mangrove wetland, Plant Soil, 473, 489–505, https://doi.org/10.1007/s11104-022-05300-z, 2022.